JOURNAL OF APPLIED ELECTROCHEMISTRY 18 (1988) 679–686

Kinetics of formic acid oxidation in advanced porous electrodes

RUDOLF HOLZE

*Institut für Physikalische Chemie der Universität Bonn, Wegelerstr. 12, D-5300 Bonn 1, West Germany**

ANA-MARIA CASTRO LUNA

INIFTA, Suc. No. 4 CCNo-16, 1900 La Plata, Argentina

Received 4 November 1987; revised 29 February 1988

The electrochemical oxidation of formic acid HCOOH at porous PTFE-bonded platinum–carbon electrodes in acidic electrolyte has been studied using the AC-impedance method. A reaction sequence based on known details of this process was transferred into an equivalent circuit which was used to simulate successfully the measured impedance data. The results confirm earlier data obtained with smooth platinum electrodes and allow, for the first time, a correlation between the electrode overpotential and the contribution of the various reaction steps. Further improvements of the porous electrode based on these results are suggested.

1. Introduction

Recently there has been a renewed interest in the application of the electrochemical oxidation of easily accessible organic fuels such as formic acid (HCOOH) or methanol (H_3COH) as the anodic reaction in air breathing fuel cells. This interest is based mainly on two areas of progress: firstly the improved electrocatalysis of the anodic reaction achieved by surface modification of the most commonly used electrocatalyst, platinum, or by electrochemically active species which are underpotential deposited on platinum or other catalysts (upd-metals) [1–4]; and secondly the advances in the development of platinum-free oxygen electrodes [5, 6].

In various reports on the performance of porous platinum–carbon electrodes in the presence of lead [7] or tin [8] in the electrolyte, significant improvements have been described. A further improvement in performance was achieved by Furuya and Motoo [9], who used a gas diffusion electrode as anode, where the CO_2 produced was removed on the back side of the electrode. This idea was further developed by Watanabe *et al.* [10] into a backward feed and exhaust type methanol anode. With this electrode the electrode concentration polarization usually found with porous electrodes immersed in the electrolyte is substantially reduced by supplying the fuel and removing the gaseous reaction product CO_2 from the back side of the electrode.

So far no study has been presented describing the contribution of the various steps of the electrochemical oxidation reaction to the electrode overpotential under load, in particular as a function of changing experimental parameters such as concentration of reactants or structure of the porous electrode. Thus we have attempted to measure the faradaic impedance of a working anode and to interpret these data based on a methodological approach described earlier [11–14] and applied successfully to the investigation of porous oxygen reduction electrodes [15–18].

2. Experimental details

Porous PTFE-bonded platinum–carbon electrodes of the gas fed electrode type were prepared according to a procedure described earlier [7, 12, 17]. The catalyst powder (platinum–carbon, 10% wo, HERAEUS) is dispersed in water, a PTFE dispersion (HOECHST) is added, the stirred mixture is spread on paper, pressed onto a palladium–gold metal gauze and dried. In this manufacturing process the total catalyst loading (platinum and carbon), PTFE-content of the catalyst layer and the pressure applied to the electrode were varied. Polarization curves and impedance measurements were carried out using a plexiglass cell designed according to the special requirements of AC-measurements [12]. A BANK PCA 72 M potentiostat, a home built function generator and a SOLARTRON 1172 transfer function analyser were used for the experiments. The working electrode was mounted in the cell with 1 cm^2 electrode surface exposed to the electrolyte solution, the backside of the electrode was covered with a plexiglass disc if not stated otherwise (see text below). A reversible hydrogen electrode, as suggested by Will [19], was used as a reference electrode. Since a counter electrode, where hydrogen evolution might take place, was undesirable because of possible diffusion of hydrogen to the working electrode under study, an oxygen consuming porous gas-fed electrode was used as a counter electrode. All measurements were made at room temperature. Electrolyte solutions were prepared from $HClO_4$ (1 M,

---

* New Address: Universität Oldenburg, Fachbereich Chemie, Carl-von-Ossietzky-Str. 9-11, D-2900 Oldenburg, West Germany.

MERCK, pA) and various concentrations of formic acid (MERCK). In some experiments 1×10^{-4}M $Pb(ClO_4)_2$ was added to the solution. The electrolyte solutions were purged with nitrogen in order to remove traces of oxygen which might establish a mixed electrode potential at the anode.

The electrode impedance was measured over a frequency range from 1 mHz to 10 kHz. The electrolyte resistance, R_{sol} (later used for the iR drop correction in the measurements of polarization curves) and the double layer capacity, C_{dl}, were calculated according to procedures already described [12] and subtracted from the measured electrode impedance. Using appropriately selected equivalent circuits the faradaic impedance obtained in this way was simulated with a non-linear least square fit using the Marquardt-Levenberg algorithm [12, 16, 20, 21] incorporated into the subroutine ZXSSQ supplied by the International Mathematic and Statistic Library, IMSL.

3. Results and discussion

3.1. *Optimization of the electrode*

A set of polarization curves of electrodes prepared with various applied pressures is presented in Fig. 1. It shows an optimum pressure around 250 bar, at lower pressures the performance at high current densities (*cd*) drops, presumably due to poorer conductivity of the electrode and increasing diffusion polarization inside the porous structure. A higher pressure results in an electrode of lower catalytic activity (more positive rest potential), nevertheless the electrode performance approaches the values of the 'optimum' electrode, which already indicates that the electrochemical reaction takes place mostly on the outer side of the porous electrode. The double layer capacity data derived from the electrode impedance rises from $C_{dl} = 112\,\mu F\,cm^{-2}$ at $p = 75$ bar to $C_{dl} = 124\,\mu F\,cm^{-2}$ at $p = 150$ bars and $C_{dl} = 125\,\mu F\,cm^{-2}$ at $p = 250$ bars. At higher pressures a further increase to $C_{dl} = 248\,\mu F\,cm^{-2}$ at 400 bars is observed. The electrochemically active surface area (covered with organic adsorbate) seems to be reflected in the C_{dl} values: a lower value indicates a lower active surface area and consequently a poorer electrode performance at low *cd*, where the electrode potential is mostly determined by electrocatalysis. At higher current densities this difference is diminished and other factors like electronic conductivity of the electrode are important. This has been observed in several cases with porous PTFE-bonded electrodes [12, 17]. Nevertheless these values of C_{dl} do not represent directly either the internal surface area of the porous electrode wetted with electrolyte solution or the electrochemically active surface area [12, 15, 17]. In the case of these electrodes, when used as oxygen reducing cathodes in the absence of organic fuels in the electrolyte, values of $C_{dl} = 2\,mF\,cm^{-2}$ (per geometric surface area of the electrode) were measured. The values of C_{dl} obtained here are much smaller due to adsorption of organic molecules [23].

These results suggest that, strictly speaking, an increase of the catalyst loading (total of platinum and carbon cm^{-2}) should lead to an improved electrode performance preferably at low *cd*s, where the potential is under activation control, whereas at higher *cd*s the difference should disappear. This is supported by the results in Fig. 2, although the difference between the two electrodes is still significant (100 mV) at the highest *cd* measured. This indicates that either, even at this *cd*, there is still mixed activation and transport control of the electrode potential or that there are further effects of the changed catalyst loading influencing the electrode properties. The difference between the two electrodes is not reflected in the double layer capacity; at both loadings the values of C_{dl} are roughly equal when a pressure of 150 bar or 250 bar is applied during the manufacture of the electrode.

A similar effect is observed when the PTFE-content is reduced. Considering the hydrophobic properties of this binding agent a reduction of its content in the

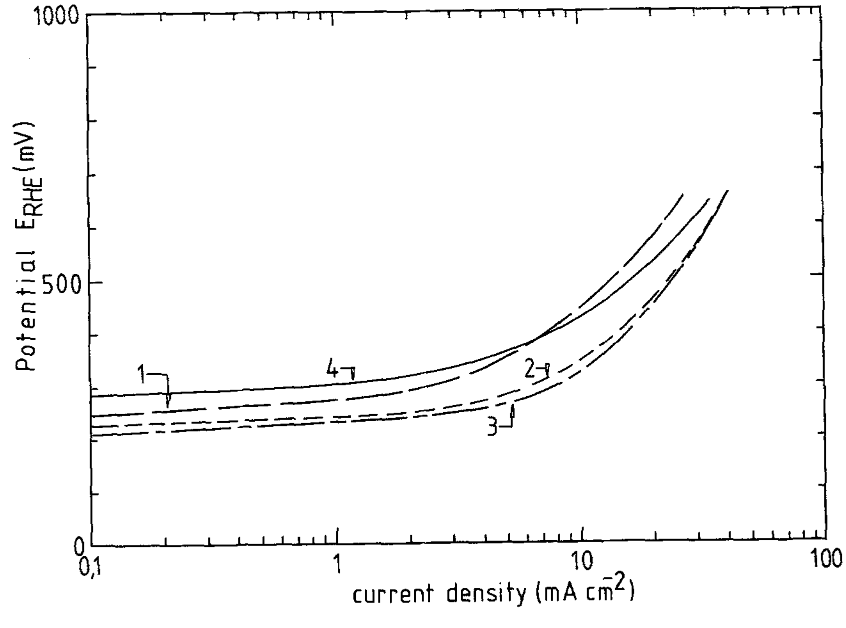

Fig. 1. Current density against potential curves for platinum–carbon anodes prepared with different pressures applied to the electrode (1) 75 bar, (2) 150 bar, (3) 250 bar, (4) 400 bar, 1 M HCOOH, 1 M $HClO_4$, room temperature, corrected for iR-drop.

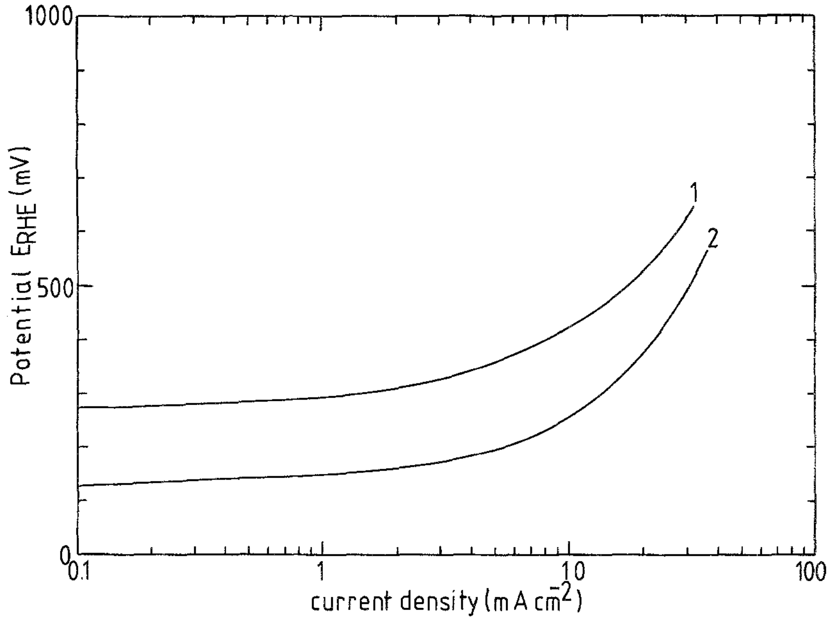

Fig. 2. Current density against potential curves for platinum–carbon anodes prepared with different total catalyst loadings of (1) 14 mg cm^{-2} Pt/C and (2) 20 mg cm^{-2} Pt/C, 1 M HCOOH, 1 M $HClO_4$, room temperature, corrected for iR-drop.

electrode should result in a less hydrophobic and, consequently, more flooded electrode. The results support this view. The double layer capacity is greatly enhanced. In addition, the rest potential, E_0, is shifted from $E_0 = 736\,mV_{RHE}$ at a PTFE-content of 42% wo to $E_0 = 112\,mV_{RHE}$ at a PTFE-content of 26% wo.

A preliminary optimization of the electrode structure thus leads to the following manufacturing parameters: pressure 250 bar, PTFE-content 26% wo and 20 mg cm^{-2} catalyst loading. Using these electrodes the influence of the fuel concentration and the addition of Pb^{2+} to the electrolyte solution was studied.

The influence of the formic acid concentration upon the polarization curve is evident from Fig. 3. With increasing concentration of HCOOH the performance is improved significantly. This indicates a major influence of this concentration upon the electrode overpotential under load.

A major gain in electrode performance has been reported after addition of small amounts of metal ions capable of upd deposition on platinum. First results obtained with porous platinum–carbon electrodes have been reported by Adzić [8] and Castro Luna *et al.* [7]. In Fig. 4 a comparison of the electrode performance with and without lead present in the electrolyte solution is given. These curves represent a further improvement in terms of overall performance; the gain amounts to about 100 mV when compared to the results of Adzić [8] (obtained with POWERCAT (Stonehart Assoc., platinum–carbon) and upd-tin) and about 100 mV when compared with the previous results of Castro Luna *et al.* [7] (obtained with a somewhat lower platinum content of presumably 5% wo and a total loading of only14 mg cm^{-2}).

Based on the suggestions of Furuya and Motoo [9] the polarization curves of our electrodes in the 'gas diffusion' mode were measured, with the back side of the electrode either exposed to ambient air or to a continuous purge flow of nitrogen. Since the electrodes under investigation here are used in appli-

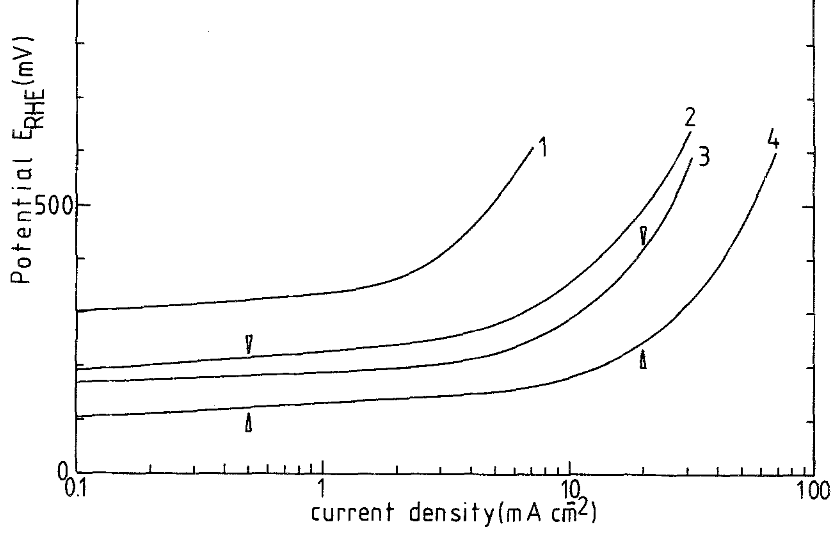

Fig. 3. Current density against potential curves for platinum-carbon anodes in 1 M $HClO_4$ electrolyte solution with various concentrations of HCOOH: (1) 0.1 M, (2) 0.5 M, (3) 1.0 M, (4) 2.0 M; room temperature, corrected for iR-drop, arrows indicate *cd* where impedance measurements were made.

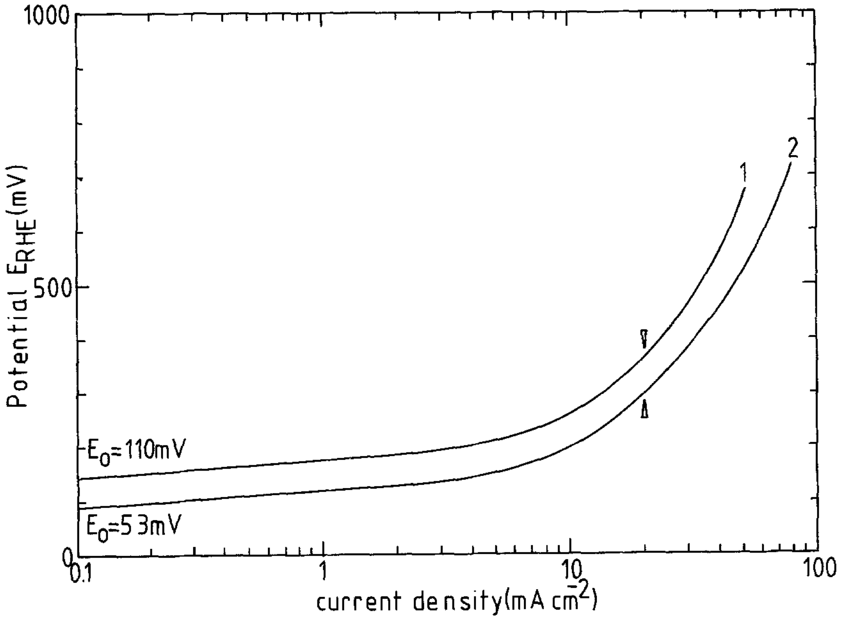

Fig. 4. Current density against potential curves for platinum–carbon anodes in 1 M $HClO_4$ and 1 M HCOOH electrolyte solution, without lead ions being present in the solution (1) and with 1 × 10^{-4}M $Pb(ClO_4)_2$ in solution, room temperature, corrected for iR-drop, arrows indicate *cd* where impedance measurements were made.

cations without positive pressure on the gas side, they are equipped with a porous PTFE–backing, acting as a hydrophobic gas transport layer. If a small gas pressure is applied the backing is no longer needed. Both types of electrode were tested.

In the case of the electrode with backing exposed to ambient air a rather poor polarization curve (see Fig. 5) was obtained. Presumably a mixed electrode potential, involving both formic acid oxidation and oxygen reduction, is established. A very similar, although not as pronounced, effect has been observed previously during the investigation of oxygen cathodes for fuel cells with organic fuels [5]. This assumption is supported by the result obtained with an electrode where the back side is purged with nitrogen (see Fig. 5). A further improvement is obtained if the backing of the electrode is omitted, especially at higher *cd*. This may be due to an enhanced flow of CO_2 out of the electrode. In addition, the partial coverage of active electrode sites by CO_2 is decreased, since the internal CO_2 pressure is reduced. By comparison with the corresponding curve (1) in Fig. 4 it is evident that the gain in performance obtained by the backward exhaust is rather small and visible mainly at higher *cd*. With combinations of this type of electrode and an appropriately modified catalyst (upd-lead modified platinum) a further improvement is to be expected. Currently, life-time testing of these electrodes is being carried out; results will be reported soon.

3.2. *Impedance measurements*

In order to obtain more quantitative data on the influence of formic acid concentration and the presence of lead on the electrode reaction kinetics, impedance measurements were performed with the electrodes of Fig. 3 and Fig. 4 at points on the current–potential curve indicated by arrows in the corresponding figures.

In order to make correlations between the elements of the equivalent circuit and the values of the impedance elements extracted from the measured impedance,

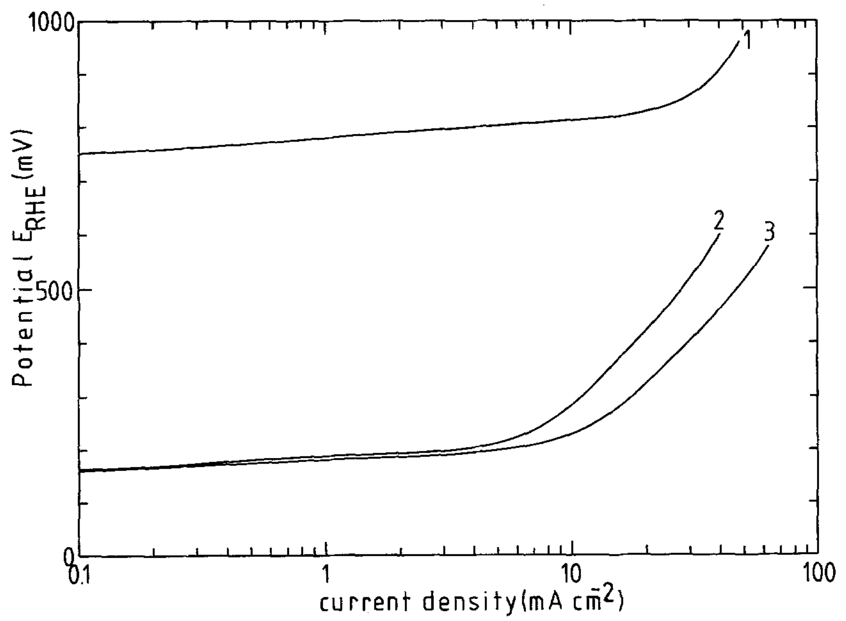

Fig. 5. Current density against potential curves for platinum–carbon anodes in 1 M $HClO_4$ and 1 M HCOOH electrolyte solution, (1) with porous PTFE-backing, electrode back side exposed to air, (2) with porous PTFE-backing, electrode back side exposed to flowing nitrogen, (3) without porous PTFE-backing, electrode back side exposed to flowing nitrogen, room temperature, corrected for iR-drop.

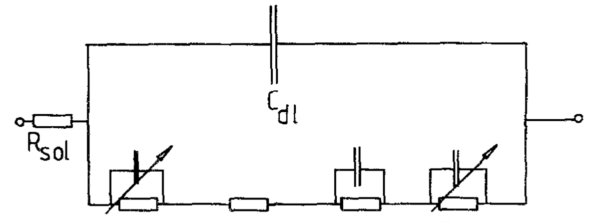

Fig. 6. Equivalent circuit of a working anode, Z_{diff1} = diffusion impedance of the HCOOH-diffusion, R_{ct} = charge transfer resistance, R_{ads} and C_{ads} adsorption impedance of the dissociative chemisorption of HCOOH on the electrode, Z_{diff2} = diffusion impedance of the product (CO_2) diffusion, C_{dl} = double layer capacitance, R_{sol} = electrolyte solution resistance (further discussion see text).

the current density and the concentration of HCOOH were varied.

The equivalent circuit was based on a reaction sequence as follows:

- diffusion of the reactant HCOOH to the reaction site (the porous electrode)
- adsorption or surface chemical reaction. According to the literature (see below) a dissociative chemisorption has to be assumed as the first reaction step
- charge transfer, presumably attributed to the oxidation of the absorbed hydrogen formed in the preceding step
- diffusion of reaction products (CO_2 in the acidic electrolyte solution under study)

This model does not include the further reactions of the absorbates, with the exception of the charge transfer due to the oxidation of the adsorbed hydrogen, since further reaction results in the formation of additional adsorbed hydrogen, which is also oxidized (this cannot be separated from the oxidation process mentioned above). This reaction was assumed to be even faster than the first step [22] and was not included in the equivalent circuit. The final oxidation step of the carbonaceous adsorbate on the electrode is extremely slow [24] and its contribution could not be detected in the measured electrode impedance. The resulting equivalent circuit, based on this sequence including the double layer capacitance C_{dl} of the electrode and the electrolyte resistance R_{sol} present between the tip of the Luggin capillary and the surface of the working electrode, is given in Fig. 6.

A set of data describing the impedance element of this equivalent circuit as obtained with an electrode of the optimized type described above and measured in an electrolyte solution at a current density of $5\,\mathrm{mA\,cm^{-2}}$ and $20\,\mathrm{mA\,cm^{-2}}$ with various concentrations of HCOOH, is given in Table 1. The measured and the fitted electrode impedance are presented in Figs 7a, b and c. The most significant change of parameters observed as a function of HCOOH concentration is the changed magnitude of the diffusion factor $A1$ and the diffusion resistance R_{diff1}. According to the equations of the Nernstian diffusion the impedance Z_{diff} is given by:

$$Z_{diff} = R_{diff} f(x) \quad (1)$$

The diffusion resistance:

$$R_{diff} = RTd/(n^2F^2DAc_s) \quad (2)$$

where R = gas constant
T = temperature
d = thickness of the Nernst diffusion layer
n = number of electrons transferred in the rate determining step
F = Faraday constant
D = diffusion coefficient of the diffusing species
A = electrode surface
c_s = surface concentration of the diffusing species

and the diffusion function is

$$f(x) = (\sinh(x) + \sin(x)) - i\sinh(x) - \sin(x)/x(\cosh(x) + \cos(x)) \quad (3)$$

with a diffusion factor $x = 2d(\omega^{1/2})/(2D)^{1/2}$ and $i = \sqrt{-1}$. (For a detailed discussion of this impedance element as well as related impedance elements see [5, 11, 12]).

Thus a decrease of R_{diff} and $A1$ with increasing concentration of HCOOH, with all other experimental parameters kept constant, means a corresponding decrease of the diffusion layer thickness, d, and surface concentration, c_s. This diffusion impedance element describes the diffusion of the reactants to the reaction sites. The diffusion process contributes a substantial amount to the electrode overpotential, up to more than 50%. This is mainly due to the comparatively slow diffusion of HCOOH in water (the diffusion coefficient D_{HCOOH} varies from $D = 1.5 \times 10^{-5}\,\mathrm{cm^2\,s^{-1}}$ at 0.1 M concentration to $1.37 \times 10^{-5}\,\mathrm{cm^2\,s^{-1}}$ at 2 M

Table 1. Results of the fitting procedure of the parameters describing the faradaic impedance

c (M)	cd $(mA\,cm^{-2})$	$A1$[1] $(s^{1/2})$	$A2$[2] $(s^{1/2})$	R_{diff1}[3] (Ωcm^2)	R_{diff2}[4] (Ωcm^2)	R_{ads}[5] (Ωcm^2)	C_{ads}[6] $(F cm^{-2})$	R_{ct} (Ωcm^2)	k_{ads} (s^{-1})	C_{dl}[7] $(\mu F cm^{-2})$
0.5	5.0	15.0	0.056	6.36	0.199	8.35	5.46	0.110	0.02	250.0
2.0	5.0	2.8	0.09	1.36	0.3	11.70	3.90	0.180	0.02	181.0
1.0	20.0	7.31	0.079	3.36	0.23	1.05	13.30	0.167	0.07	213.0
2.0	20.0	6.52	0.065	3.07	0.24	2.02	5.33	0.138	0.09	209.0

[1] $A1$ diffusion factor associated with the diffusion of HCOOH; [2] $A2$ diffusion factor of the diffusion of CO_2; [3] R_{diff1} diffusion resistance associated with the diffusion of HCOOH; [4] R_{diff2} diffusion resistance associated with the diffusion of CO_2; [5] R_{ads} and [6] C_{ads} adsorption/reaction resistance and capacitance; [7] C_{dl} double layer capacitance.

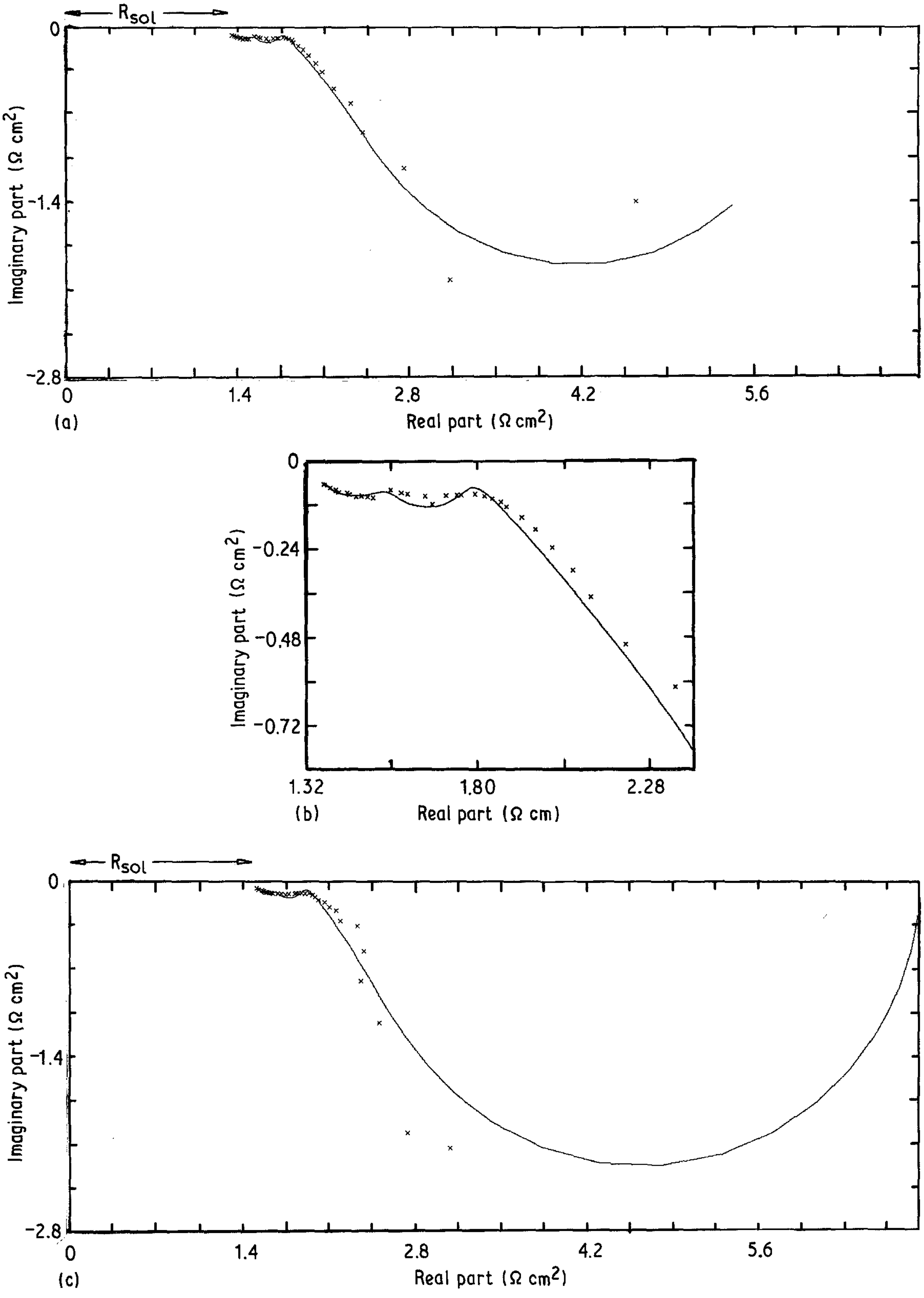

Fig. 7. Measured and calculated (fitted) electrode impedance of the electrode as described in Table 1, lines 3 and 4. $cd = 20\,\mathrm{mA\,cm^{-2}}$, concentration of HCOOH: 1 M in (a) and (b) (high frequency part only) and 2 M in (c); x = measured impedance values, (——) calculated impedance values, room temperature, for full details see Table 1 and text.

[25], which is further hindered in the present case by the fact that, in the strongly acidic $HClO_4$ solution, the formic acid remains mostly undissociated and therefore diffuses only along a concentration gradient without any migrative contribution. The second diffusion impedance, characterized by a lower diffusion resistance and a smaller diffusion factor, *A2*, is consequently associated with the diffusion of the reaction product CO_2.

From the adsorption resistance, R_{ads}, and the adsorption capacitance, C_{ads}, the rate of adsorption can be calculated [5] according to

$$k_{ads} = 1/(R_{ads}C_{ads}) \qquad (4)$$

Table 2. Results of the fitting procedure of the parameters describing the faradaic impedance

c (M)	cd ($mA\,cm^{-2}$)	$A1$ ($s^{1/2}$)	$A2$ ($s^{1/2}$)	R_{diff1} (Ωcm^2)	R_{diff2} (Ωcm^2)	R_{ads} (Ωcm^2)	C_{ads} ($F cm^{-2}$)	R_{ct} (Ωcm^2)	k_{ads} (s^{-1})	C_{dl} ($\mu F cm^{-2}$)
1.0	20.0	7.31	0.079	3.36	0.23	1.05	13.3	0.167	0.07	213.0 no lead present in the electrolyte sol.
1.0	20.0	7.49	0.090	3.69	0.24	1.04	12.6	0.130	0.07	245.0 $Pb(ClO_4)_2$ in the electrolyte sol.

Footnotes as in Table 1.

The rate constants calculated in this way are shown in Table 1. The values are somewhat higher than those previously published by Pletcher and Solis [26] with lead ions present on the electrode. This difference might be due to the fact, that the active electrode surface area of the porous electrode used here is substantially higher than the geometric surface area of 1 cm^2. Based on the double layer capacitance data a surface factor of 10 might be assumed resulting in a decrease of k_{ads} by an order of magnitude. Nevertheless, such an estimate is rather difficult due to the fact that the double layer capacitance in the presence of adsorbed organic species deviates from the values measured in the absence of such molecules (ca. $20\,\mu F\,cm^{-2}$ true surface area for a smooth metal electrode).

On addition of lead ions to the solution a further improvement of the electrode performance has been observed (see Fig. 4).

The results of the fitting procedure obtained in two measurements, with and without lead ions, are given in Table 2. No significant difference between the results can be detected; the actual differences in the values given is within the experimental margin of error. In both cases the value of k_{ads} is higher than the value calculated at lower *cd*s, since a higher *cd* corresponds to a more positive potential with a decrease in lead coverage [26]. This might explain the increase in k_{ads} as observed previously with a smooth platinum electrode [26]. Thus it can be concluded that the rate determining step in the presence, as well as in the absence of lead ions is the dissociative chemisorption of formic acid on platinum in the porous carbon electrodes used in this work. A more detailed description of the role of the lead ions, as suggested by Solis and Pletcher [26], which proposed dissociative chemisorption to occur at two platinum atoms adjacent to an adsorbed lead atom in the rate determining step, would require further measurements of parameters such as lead coverage as a function of electrode potential in the absence and presence of formic acid and as a function of time. This will be attempted in subsequent work. A comparison of the slope of the current density against potential curves in Fig. 4 shows that the slope $dE/d\,(cd)$ of the two curves, which is equivalent to the sum of the resistive components of the electrode impedance (or to $Z_{\mathrm{electr.}}$ at zero frequency [17]) is almost exactly the same. Thus the sum of the impedance elements calculated from both experiments should be the same, although a different distribution might have been possible. The potential difference between the curves is 90 mV at a *cd* of 20 mA cm^{-2}. The difference in rest potentials, E_0, is 63 mV. Various models describing the role of upd lead in formic acid oxidation electrocatalysis have been proposed. Adzić *et al.* [27] have assumed that upd lead prevents the formation of strongly adsorbed electrode poisoning intermediates by separation of platinum adsorption sites on the electrode surface. Pletcher and Solis [26] observed an increase in the rate constant of the adsorption step. The results presented here do not lend strong support to the latter model, although the uncertainties about the rate constants, corrected with respect to the true electrode surface area, do not entirely exclude their model. The model of Adzić *et al.* [27] suggests a lower coverage with strongly adsorbed intermediates, which inhibit further electrode reaction, in the presence of lead ions, which should result in a potential shift of the polarization curve to more anodic values as observed here. This model is also consistent with the impedance data reported here, since it does not assume changes in the rates of the adsorption process and the other potential determining steps.

4. Conclusions

The electrochemical oxidation of formic acid at a PTFE-bonded porous platinum carbon electrode has been investigated using the AC-impedance method. Based on the results of potential current density curves, improvements of the electrodes have been suggested. With these advanced electrodes impedance measurements showed a significant contribution of the formic acid diffusion to the working electrode overpotential. The dissociative chemisorption step preceding the charge transfer step was found to be independent on the presence of lead ions in the solution. The improvement of the electrode performance due to upd lead can be explained in terms of a model suggested by Adzić *et al.*, which assumes a decrease in coverage of the electrode with strongly adsorbed intermediates.

References

[1] D. M. Kolb, 'Advances in Electrochemistry and Electrochemical Engineering', Vol. 11 (edited by H. Gerischer and C. W. Tobias), Wiley, New York (1978) p. 125.

[2] R. R. Adzić, 'Advances in Electrochemistry and Electrochemical Engineering', Vol. 13 (edited by H. Gerischer and C. W. Tobias), Wiley, New York (1984) p. 159.

[3] G. Kokkinidis, *J. Electroanal. Chem.* **201** (1986) 217.

[4] P. C. Andricacos, M. Krishnan and D. Rath, Ext. Abstracts, 170th Electrochem. Soc. Meeting, San Diego, USA, 19–24.10.1986, 442A.

[5] R. Holze, I. Vogel and W. Vielstich, *J. Electroanal. Chem.* **210** (1968) 277 and references therein.

[6] K. A. Radyushkina and M. R. Tarasevich, *Elektrokhimiya* **22** (1986) 1155 and references therein; R. Holze, J. Ahn and W. Vielstich, DECHEMA-Monographie, in print.

[7] A. Castro Luna, T. Iwasita and W. Vielstich, *J. Electroanal. Chem.* **196** (1985) 301.

[8] R. R. Adzić, Ext. Abstracts, 167th Electrochem. Soc. Meeting, Toronto, Canada, 12–17.5.1985, 637A.

[9] N. Furuya and S. Motoo, *ibid.* **179** (1984) 303.

[10] M. Watanabe, M. Uchida and S. Motoo, *J. Electroanal. Chem.* **199** (1986) 311.

[11] D. W. Wabner, Habilitation thesis, München 1976.

[12] R. Holze, PhD thesis, Bonn 1983.

[13] F. Barz, J. Willsau and R. Holze, *Bull. Soc. Chim. Beograd* **48** Suppl. (1983) 339.

[14] R. Holze and W. Vielstich, *Progress in Batteries and Solar Cells* **5** (1984) 77.

[15] R. Holze and W. Vielstich, *Electrochim. Acta* **29** (1984) 607.

[16] D. Wabner, R. Holze and P. Schmittinger, *Z. Naturforsch.* **39b** (1984) 157.

[17] R. Holze and W. Vielstich, 'Advances in Battery Materials and Processes' (edited by J. McBreen, D.-T. Chin, R. S. Yeo and A. C. C. Tseung), Pennington, New Jersey (1984) p. 230.

[18] R. Holze and W. Vielstich, *J. Electrochem. Soc.* **131** (1984) 2298.

[19] F. G. Will and H. J. Hess, *J. Electrochem. Soc.* **120** (1973) 1.

[20] K. Levenberg, *Quart. Appl. Math.* **2** (1944) 164.

[21] D. W. Marquardt, *J. Siam* **11** (1963) 2.

[22] W. Vielstich, 'Fuel Cells', Wiley-Interscience, London (1970).

[23] B. B. Damaskin, O. A. Petrii and V. V. Batrakov, 'Adsorption organischer Verbindungen an Elektroden', Akademie-Verlag, Berlin 1975.

[24] A. Capon and R. Parsons, *J. Electroanal. Chem.* **45** (1973) 205.

[25] L. A. Dunn and R. H. Stokes, *Australian J. Chem.* **18** (1965) 285.

[26] D. Pletcher and V. Solis, *J. Electroanal. Chem.* **131** (1982) 309.

[27] R. R. Adzić, D. N. Simić, D. M. Drazić and A. R. Despić, *J. Electroanal. Chem.* **61** (1975) 117; **65** (1975) 587; **80** (1977) 81.